Inflammatory Bowel Diseases, 2022, **28**, 1485–1496
https://doi.org/10.1093/ibd/izac098
Advance access publication 23 May 2022
Leading Off

Molecular Network Analyses Implicate Death-Associated Protein Kinase 3 (DAPK3) as a Key Factor in Colitis-Associated Dysplasia Progression

Huey-Miin Chen, PhD, and Justin A. MacDonald, PhD

From the Department of Biochemistry & Molecular Biology, Cumming School of Medicine, University of Calgary, Calgary, Canada

Address correspondence to: Justin A. MacDonald, PhD, Department of Biochemistry & Molecular Biology, University of Calgary, 3280 Hospital Drive NW, Calgary, AB, T2N 4Z6 (jmacdo@ucalgary.ca).

Background: Ulcerative colitis (UC) is a progressive disorder that elevates the risk of colon cancer development through a colitis-dysplasia-carcinoma sequence. Gene expression profiling of colitis-associated lesions obtained from patients with varied extents of UC can be mined to define molecular panels associated with colon cancer development.

Methods: Differential gene expression profiles of 3 UC clinical subtypes and healthy controls were developed for the GSE47908 microarray data set of healthy controls, left-sided colitis, pancolitis, and colitis-associated dysplasia (CAD) using limma R.

Results: A gene ontology enrichment analysis of differentially expressed genes (DEGs) revealed a shift in the transcriptome landscape as UC progressed from left-sided colitis to pancolitis to CAD, from being immune-centric to being cytoskeleton-dependent. Hippo signaling (via Yes-associated protein [YAP]) and Ephrin receptor signaling were the top canonical pathways progressively altered in concert with the pathogenic progression of UC. A molecular interaction network analysis of DEGs in left-sided colitis, pancolitis, and CAD revealed 1 pairwise line, or edge, that was topologically important to the network structure. This edge was found to be highly enriched in actin-based processes, and death-associated protein kinase 3 (DAPK3) was a critical member and sole protein kinase member of this network. Death-associated protein kinase 3 is a regulator of actin-cytoskeleton reorganization that controls proliferation and apoptosis. Differential correlation analyses revealed a negative correlation for *DAPK3-YAP* in healthy controls that flipped to positive in left-sided colitis. With UC progression to CAD, the *DAPK3-YAP* correlation grew progressively more positive.

Conclusion: In summary, DAPK3 was identified as a candidate gene involved in UC progression to dysplasia.

Lay Summary

Our investigation verified pancolitis as a conduit for ulcerative colitis advancement from left-sided colitis to dysplasia and uniquely identified dysregulation of actin reorganization, with death-associated protein kinase 3 and Yes-associated protein as key molecular determinants for disease progression.

Key Words: death-associated protein kinase, zipper-interacting protein kinase, differential-gene expression, ulcerative colitis, dysplasia, colon cancer

Introduction

Ulcerative colitis (UC) is a chronic, inflammatory bowel disease (IBD) that is confined to the mucosal layer of the large bowel, most commonly the rectum, and may extend proximally in a continuous fashion.[1] This is a heterogeneous and progressive disorder that has seen a substantial increase in its global prevalence. The current framework of UC pathogenesis comprises environmental, genetic, immune, and microbiome factors that culminate at the perturbation of the mucosal barrier and prolonged mucosal inflammatory response.[2] Consequently, UC is a clinically, molecularly, and genetically heterogeneous disease that fosters varied disease courses and mixed responses to therapy.[3] The genetic heterogeneity is highlighted in the analysis of 75 000 IBD cases and controls by Jostins and colleagues[4] that identified 23 UC-specific risk loci with primary involvement in the regulation of the epithelial barrier function and immune pathways. Genetic studies such as this promote the concept that UC disease susceptibility is a compilation of small effects or gene alterations that are not shared by all patients.

Ulcerative colitis patients are at greater risk of developing colitis-associated colorectal cancer (CAC) through an acceleration of the colitis-dysplasia-carcinoma sequence of cellular transformation.[5–7] Although the probability of developing CAC appears to have declined, likely due to advancements in medical therapies and/or optimizations in endoscopic surveillance, CAC remains a dire consequence of long-standing UC.[5,8] While frequent surveillance can reduce the CAC incidence and mortality in patients with IBD,[9] surveillance of IBD patient cohorts is challenged by concomitant inflammation, scarring, and flat dysplasia with indistinct margins.[10] The burden of colonoscopy surveillance may be eased with the discovery of biomarkers that can be routinely used to identify patients at high risk of developing dysplasia or CAC.

A mutational signature analysis of tissue and blood samples from CAC patients showed that the evolutionary

Received for publication: October 31, 2021. Editorial Decision: April 14, 2022

trajectory of disease is initiated early in the colitis-dysplasia-carcinoma sequence.[11] Furthermore, the extent of colitis has been recognized as an independent risk factor, and the most significant risk factor, for CAC.[12] In support of this, Bjerrum and colleagues[13] provided transcriptional profiles of colonic mucosa from patients with varying extents of UC. A gene expression data set (GSE47908) was generated from mucosal biopsies sampled from the left colon of patients with left-sided colitis, pancolitis, or colitis-associated dysplasia (CAD), plus from healthy controls (HC). The authors identified differential transcriptional profiles aligned with the UC extent (i.e., areas of involvement) that were not inferred by potential covariates in the clinical data (i.e., age, years with disease, Mayo score, and medication). Their findings suggest that gene expression profiles of colitis-associated lesions obtained from patients with varied extents of UC can be mined to support the development of molecular panels that identify patients at high risk of developing CAD or CAC.[13] However, additional network analyses and detailed mechanistic interrogations of specific molecular participants were not completed.

Elucidation of the mechanisms of colon carcinogenesis requires further investigation, and insight into the molecular events underpinning the progression of UC to colitis-associated colon cancer may be gained from the study of nondysplastic colonic mucosa.[11,13] The transcriptional data set generated by Bjerrum and colleagues[13] provides an excellent resource to perform such an analysis. In this study, we performed a differential expression analysis, pathway and network analyses, and a differential correlation analysis on the GSE47908 data set to determine how the extent of colitis impacts upon biological functions and regulatory pathways and to identify the key molecular factors that bridge the colitis-dysplasia progression. The results provide insight into the molecular events associated with colitis-dysplasia progression, which could be exploited for the development of biomarkers in nondysplastic mucosa that identify the risk of dysplasia for UC patients.

Methods

Data Processing

Data processing was completed using the R (v4.0.2; R Studio) programming language, and all codes used in this study align with recommendations made by authors of R packages in their respective user guides, which can be accessed at https://bioconductor.org.

Differential Gene Expression Analysis

Log-transformed microarray expression data for GSE47908 and microarray platform data for GPL570 (HG-U133_Plus_2; Affymetrix Human Genome U133 Plus 2.0 Array) were retrieved from the Gene Expression Omnibus (GEO) database, available at https://www.ncbi.nlm.nih.gov/geo/ with the R package GEOquery. The limma R workflow[14] was used to detect differentially expressed transcripts between the UC clinical subtypes [left-sided colitis (n = 20), pancolitis (n = 19), CAD (n = 6)], and HC (n = 15) samples]. Specifically, the function |lmFit| was used to generate a linear model fit to the data matrix containing log expression values for GSE47908. Next, function |contrasts.fit| was used to compute estimated coefficients and standard errors for a given set of contrasts (e.g., pancolitis versus HC). Finally, function |eBayes| was used to compute log-odds of differential expression by empirical Bayes moderation of the standard errors towards a global value. All functions were operated with default settings.

Log-fold changes calculated by function |eBayes| for 54 675 transcripts, along with their false discovery rates (FDRs) and P values, were uploaded to the Ingenuity Pathway Analysis (IPA) software (Qiagen Inc., Redwood City, CA, USA). Some transcript identifiers remain unmapped by IPA; these genes were eliminated from the study, leaving 45 480 transcripts to be mapped. Due to redundancy of the GeneChip HG-U133 Plus 2.0 Array (Affymetrix Inc., Santa Clara, CA, USA), this transcript pool included duplicate genes. To resolve duplicates, IPA core analyses were performed on the mapped transcripts, and transcript identifiers were consolidated using their $\log_2$ fold change (FC) measurement, through which a representative transcript was selected based on the maximum absolute FC. This returned 21 475 "analysis-ready" genes. To distinguish the differentially expressed genes (DEGs), the combined application of a stringent FDR threshold ($q < 0.001$) and a moderate fold-change threshold ($FC > 0.75$) was used. This reduced the number of false positives while maintaining the "ideal" data set size (200–3000 genes) for a subsequent IPA core analysis of gene expression data. Differential expression was then visualized via the EnhancedVolcano R package.

Functional Analysis of DEGs in UC Disease Subtypes

To compare DEGs and illustrate possible relationships between left-sided colitis, pancolitis, and CAD, a Venn diagram was first used to visualize the overlap of DEGs found in the 3 UC clinical subtypes. The lists of overlapping DEGs derived from the comparison of UC subtypes were then used as input data for a gene ontology (GO) enrichment analysis, performed with the topGO R package (https://bioconductor.org). We chose topGO owing to its "*elim*" method, which takes GO hierarchy into consideration when calculating enrichment. For the enrichment analysis, the background consisted of all genes assessed by the microarray platform GPL570, and annotation was completed with the R package org.Hs.eg.db; GO terms with <10 annotations were excluded for interpretability. The degree of enrichment was reported as the odds ratio, where I^A equals the number of DEGs annotated with the GO term, I^B equals the number of background genes annotated with the GO term, and the odds ratio was calculated as (I^A ÷ size of DEG list) ÷ (I^B ÷ size of background list). Statistical significance was defined with a Fisher's exact test.

Ingenuity Pathway Analyses

To analyze changes in biological states across the UC clinical subtypes, 3 sets of IPA Core Analyses were performed, followed by an IPA comparison analysis. The IPA comparison analysis allows for the side-by-side comparison of multiple core analyses, which facilitated the discovery of trends amongst the 3 data sets. Core analyses were performed on the 3 data sets (i.e., left-sided colitis versus HC, pancolitis versus HC, and CAD versus HC) to assess the canonical pathways, upstream regulators, molecular and cellular functions, and molecular interaction networks that were most likely to be perturbed based on the changes in gene expression. Within the IPA, canonical pathways were built with reference to literature prior to the DEG input, and did not undergo structural changes upon the DEG input. Instead, the IPA computes a z-score that assesses the directionality within a gene set (i.e.,

the DEG input) to infer the activation state of each canonical pathway or molecular and cellular function. Upstream regulators were identified by the observed differential regulation of known downstream effector(s). The z-score determines the activation state of an upstream regulator by the regulation direction associated with the relationship from the upstream regulator to the effector(s). A negative z-score indicates inhibition, and a positive z-score indicates activation. Significance was calculated with the right-tailed Fisher's exact test. Changes in activation states across UC subtypes were assessed with a comparison analysis (sort method = trend + z-score). The correlation of the activation state with the extent of disease as it progressed from left-sided colitis to pancolitis to CAD (the trend) was examined, and the findings were reported as trending towards activation or trending towards deactivation.

Mapping Molecular Interaction Networks

Differentially expressed genes from the 3 data sets were mapped to their corresponding gene objects in the Ingenuity Knowledge Base (IKB), and those that interacted with other molecules in the IKB were designated as focus molecules. Focus molecules were then assembled into networks by maximizing their interconnectedness with each other (relative to the nonfocus molecules they are connected to in the IKB). While nonfocus molecules from the IKB may be used to merge smaller networks into a larger network, networks are scored based on the number of focus molecules they contain. The network size, the total number of focus molecules analyzed, and the total number of molecules in the IKB that could be included in the networks also contribute to the network scores. The score is a test of significance using hypergeometric distribution and is calculated with the right-tailed Fisher's exact test (score = –log Fisher's P value; a score ≥ 2 equals a P value ≤ .01). For this study, networks were limited to 70 molecules each, and a maximum of 25 networks per UC subtype were constructed. Individual networks (child networks, $n = 75$) were overlapped with each other to create a single parent network by virtue of common network molecules between child pairings; this was done with the RVenn R package. Finally, the edge-betweenness parameter for the core network was computed via the NetworkAnalyzer app, included in Cytoscape v3.8.0 (Cytoscape Consortium; https://cytoscape.org).

Differential Correlations

A ggplot2-based R package, ggpubr (https://rpkgs.datanovia.com/ggpubr/), was used to investigate the relationship between the expression profiles of 2 genes. A Shapiro-Wilk normality test was conducted to refine probe-set redundancies for Yes-associated protein (*YAP*) and death-associated protein kinase 3 (*DAPK3*) probe sets prior to completing the parametric correlation analyses (Figure S1). Specifically, function |stat_cor| was used to calculate the Pearson correlation coefficient. The size of the concentration ellipse in normal probability was left at the default of 0.95, which translates to a 95% confidence interval.

Results

Analysis of Genes Differentially Expressed in UC Disease Subtypes

The distributions of gene expression ratios (log-transformed) calculated between UC subtypes and HC are presented in Figure 1A. For the left-sided colitis versus HC comparison, 1016 genes had an FC greater than 0.75 ($q < 0.001$); of these DEGs, 614 were upregulated and 402 were downregulated. Pancolitis returned 2858 DEGs, half of which were upregulated. Colitis-associated dysplasia returned 1842 DEGs, of which 393 were upregulated and 1449 were downregulated.

For functional predictions, a Venn diagram was first used to identify genes with expression regulation observed in multiple UC disease subtypes (Table S1). As presented in Figure 1B, pancolitis overlapped both left-sided colitis and CAD in terms of common DEGs. Of the 2858 pancolitis DEGs, 651 shared similar expression regulation as left-sided colitis DEGs (465 common upregulation plus 159 common downregulation), and 1194 shared similar expression regulations as CAD DEGs (209 common upregulation plus 985 common downregulation). This feature was not observed when comparing left-sided colitis and CAD; less than 2% of the input DEGs appeared at the intersection of left-sided colitis ∩ pancolitis ∩ CAD. This analysis suggests pancolitis exists as the middle ground of UC subtypes and bridges the progression of UC from left-sided colitis to CAD. Thus, the DEGs located at the intersection of pancolitis ∩ left-sided colitis or pancolitis ∩ CAD were selected for the functional analysis.

To identify the potential biological processes associated with UC clinical progression, 2 sets of DEGs at the intersection of either pancolitis ∩ left-sided colitis or pancolitis ∩ CAD were processed separately with the topGO R package for the functional enrichment analysis. These enrichment analyses included both upregulated and downregulated genes. The top 10 terms from the biological process category of the GO enrichment analysis are presented in Figure 2. The DEGs at the intersection of pancolitis and left-sided colitis were enriched in inflammatory processes (Table S2), while the pancolitis ∩ CAD overlapping DEGs were enriched in actin-based processes (Table S3). Specifically, the pancolitis ∩ left-sided colitis DEGs showed significant enrichment for the regulation of interferon γ–mediated signaling pathways (GO:0060334), the antimicrobial humoral immune response mediated by antimicrobial peptide (GO:0061844), and the acute-phase response (GO:0006953), with 8.6-, 6.4-, and 6.0-fold enrichments, respectively. Across the pancolitis ∩ CAD DEGs, microvillus assembly (GO:0030033), Golgi to plasma membrane transport (GO:0006893), and actin cytoskeleton reorganization (GO:0031532) were found to be significantly over-represented, with 6.3-, 3.1-, and 3.0-fold enrichments, respectively. Overall, the GO enrichment analysis suggests that as UC progressed from left-sided colitis to pancolitis to CAD, the transcriptome pattern also shifted from being immune-centric to having cytoskeleton dependence. Presumably, the regulation of actin cytoskeleton organization plays an important role in colitis-dysplasia progression.

Association of Hippo Signaling Activation with Colitis-Dysplasia Progression

To identify the canonical pathways that are most relevant to the observed shift in the gene expression profile, a comparison analysis heat map for the canonical pathways significantly altered by UC disease subtypes was constructed (Figure 3A). This heat map displays the trend of either activation or deactivation as the gene expression profile shifted in response to the UC extent: that is, from left-sided colitis

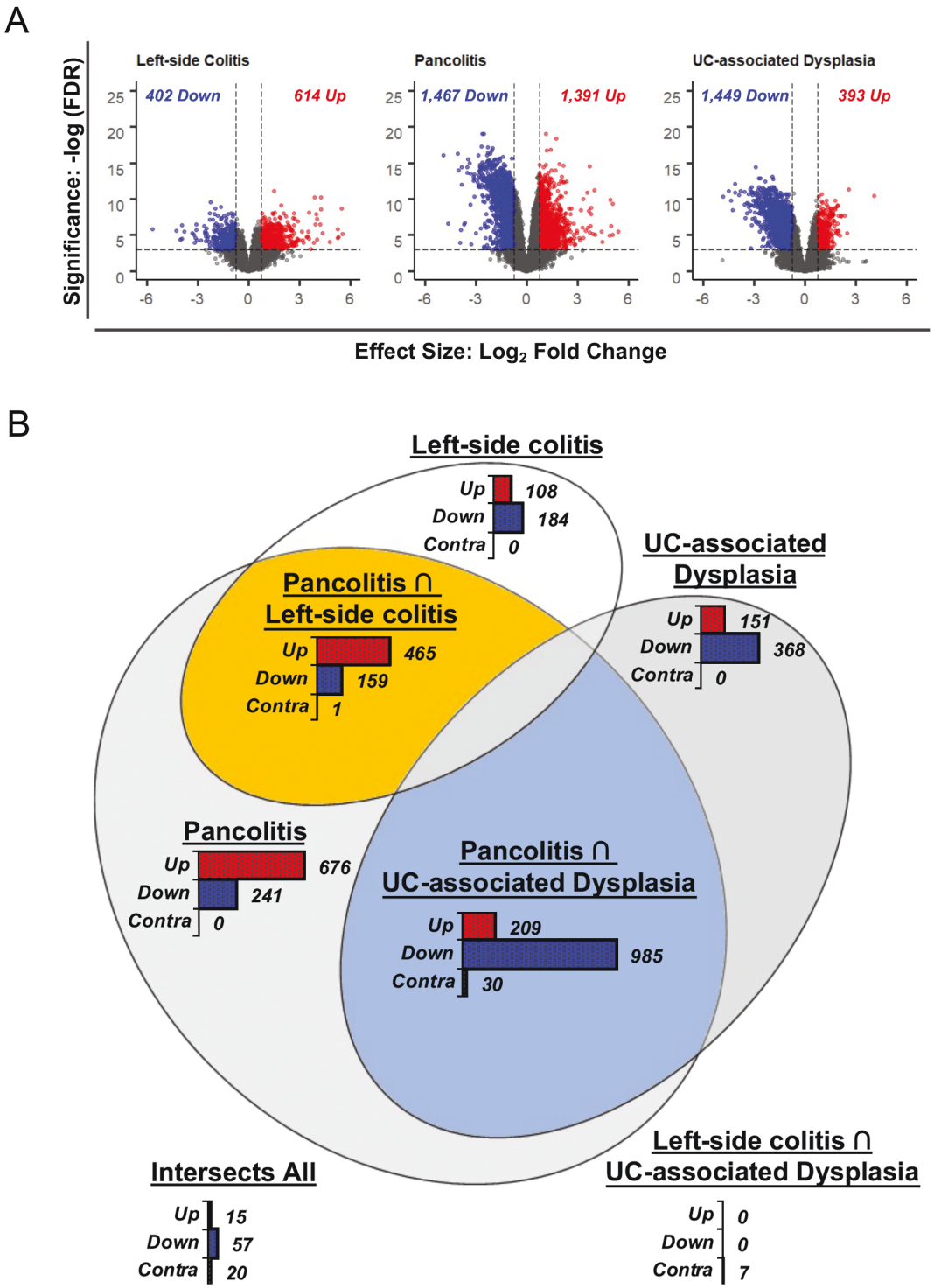

Figure 1. Differential expression of genes in UC disease subtypes. A, Differential gene expression of 3 UC clinical subtypes against HC. The FCs were calculated with limma R for the GSE47908 data set (n = 15 HC; n = 20 left-sided colitis patients; n = 19 pancolitis patients; and n = 6 CAD patients). The threshold set for FC was 0.75. Significance was determined by an FDR < 0.001. B, Overlap of shared DEGs between UC subtypes. The proportional Venn diagram was generated with Bio Venn and then optimized with eulerAPE_3.0.0.jar. Abbreviations: CAD, colitis-associated dysplasia; DEG, differentially expressed gene; FC, log2 fold-change; FDR, false discovery ratio; HC, healthy controls; UC, ulcerative colitis.

to pancolitis to CAD. The heat map revealed Hippo signaling and Ephrin-receptor signaling as the top canonical pathways that were progressively altered in concert with the pathogenic progression of UC. The Hippo-signaling pathway displayed incremental activation, while the Ephrin-receptor-signaling pathway exhibited gradual deactivation as the UC extent broadened (Figure 3A). Diagrammatic comparisons of Hippo and Ephrin-receptor analyses conducted on the UC-subtype DEGs are provided in Figures S2 and S3, respectively.

Trends of activation or deactivation were also probed on upstream regulators and biological functions to obtain a basic view of the molecular mechanisms underlying the extent of

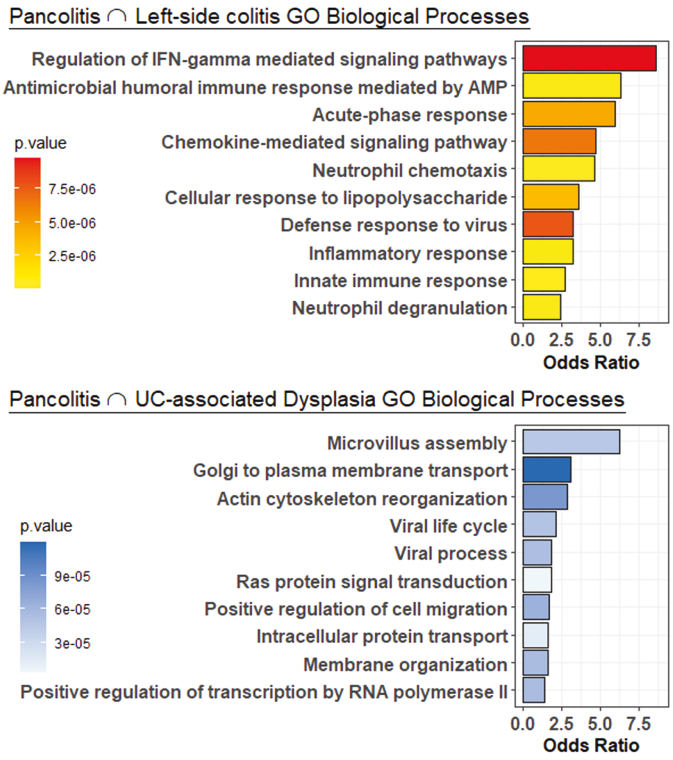

Figure 2. Gene ontology term enrichment analysis of DEGs common among UC subtypes. The DEGs at the intersection of pancolitis ∩ left-sided colitis or pancolitis ∩ CAD were subjected to GO term enrichment analysis for Biological Process categories. Enrichment was performed with topGO R ("elim" algorithm, "fisher" statistic). Statistical significance was defined with a Fisher's exact test. Abbreviations: AMP, adenosine 5′-monophosphate; CAD, colitis-associated dysplasia; DEG, differentially expressed gene; GO, gene ontology; IFN, interferon; UC, ulcerative colitis.

colitis (Figure 3B). In terms of upstream regulators, interleukin 10RA exhibited a trend of increased activity, whereas interferon γ exhibited a trend of decreased activity. Affected biological functions include apoptosis and cell movement, which underwent gradual activation and deactivation, respectively, as disease extended from left-sided colitis to pancolitis to CAD.

Actin Reorganization as a Potential Key Determinant for Colitis Progression

Using the limma R-derived DEGs, the IPA software generated 25 networks for each of the 3 UC subtypes. Molecular network intersections, assembled with the RVenn R package, revealed a single parent network that connected all 75 child networks via 757 intersections or edges (Figure 4A). Among the 75 child networks, approximately two-thirds (48/75) were composed of less than 60 focus molecules (<85% focus molecules). The 757 intersections or edges that connected the child networks each comprise 1 to 24 common molecule overlaps. Nevertheless, over half (57%) of the interactions or edges were enabled by just 1 common molecule, and 87% of the edges involved fewer than 4 common molecules (<5% overlap). To reduce noise from the parent network depicted in Figure 4A, the molecular network intersection was compiled once more, but with child networks that were built upon 60 or more focus molecules (>85% focus molecules) and preserving connections that were maintained by 4 or more common molecules (>5% overlap). This produced 1 core network of networks that connected 21 child networks with 21 edges. One intersection segment, though strongly connecting pancolitis network 6 to CAD network 10 with 24 common molecules (34% overlap), stood apart from the core network of networks (Figure 4B), so was excluded from the subsequent analysis.

To pinpoint a network pairing that could be used to discern the pathways or molecular processes bridging pancolitis to CAD, the "count of overlapping molecules" and "value of edge betweenness" measures were utilized for edge evaluation. Edge betweenness reflects the amount of control that an edge exerts over the interactions of other child networks in the parent network. The edge betweenness [e = (v,w)] is defined as the number of shortest paths between 2 nodes that go through e, divided by the total number of shortest paths that go from the 2 nodes.[15,16] Edge betweenness does not consider the number of overlapping molecules that contribute to the intrinsic strength of each edge. Thus, additional consideration for this attribute was completed post hoc. As shown in Figure 4B, the edge connecting pancolitis network 15 to CAD network 1 stood out from the remaining network associations by virtue of its large number of overlapping molecules (20% overlap) and high value of edge betweenness (Table S4). Taken together, the findings suggest that the removal of this edge may affect interactions between the remaining networks within the parent network. Thus, the overlap between pancolitis network 15 and CAD network 1 was selected for a further, detailed examination.

The intersection pancolitis 15 ∩ CAD 1 was formed by 14 gene products that were predominantly composed of actin-based processes when analyzed for GO term enrichment (Figure 5A). Specifically, the DEGs at this intersection showed significant enrichment for the ruffle organization (GO:0031529), the regulation of actin filament polymerization (GO:0030833), and the myofibril assembly (GO:0030239), with 66-, 33-, and 33-fold enrichments, respectively. However, within the confines of the IKB, none of the 13 focus molecules were directly linked to UC (Figure 5B). All probable shortest paths by which the focus molecules were connected to UC required at least 1 IPA-derived, intermediate node. For the majority of indirect connections, gene products β-catenin, E-cadherin, and tumor necrosis factor functioned as the IPA-derived intermediates.

Implication of DAPK3 as a Key Factor in the Colitis-Dysplasia Progression

Further dissection of pancolitis 15 and CAD 1 revealed 2 signal transduction gene products that reside in the overlap of these 2 networks (Table 1). Namely, DAPK3 was the sole protein kinase, and protein phosphatase PP1β catalytic subunit (PPP1CB) was the sole protein phosphatase. The remaining 12 gene products were categorized as either mechanochemical enzymes (i.e., motors) or scaffolding proteins involving the cytoskeleton. Both DAPK3 and PPP1CB were downregulated in pancolitis (FC: −1.08 in DAPK3; −1.56 in PPP1CB) and CAD (FC: −0.98 in DAPK3; −1.52in PPP1CB) but showed no deregulation in left-sided colitis. Presumably, DAPK3 and PPP1CB act as key factors regulating the altered molecular pathways that bridge pancolitis to CAD.

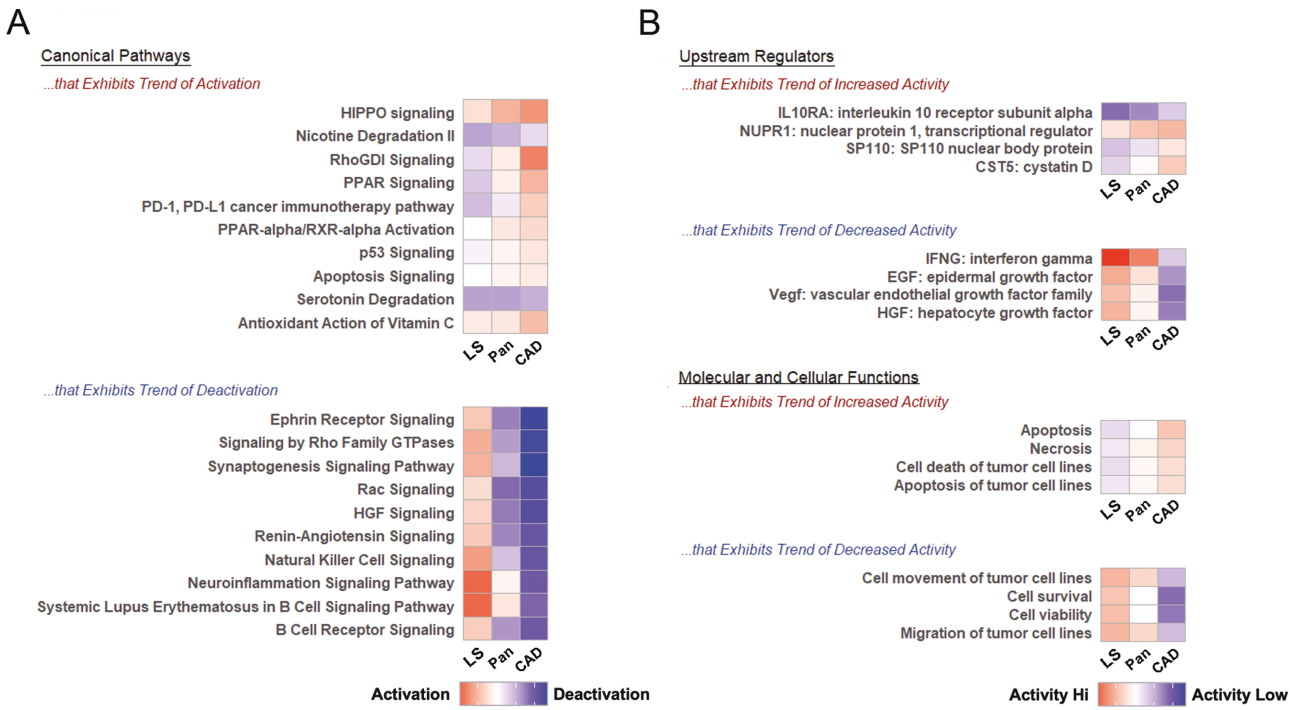

Figure 3. Ingenuity pathway analysis of canonical pathways, upstream regulators, and functions differentially deregulated among UC subtypes. For each colitis subtype, the activation z-score calculated by IPA software predicts the activation (red) or inhibition (blue) potential for each (A) canonical pathway or (B) regulator or function. The reports are sorted based on correlations of z-scores to the extent of disease (LS to Pan to CAD), with higher total scores across the colitis subtypes ranked higher than those with lower total scores. Abbreviations: CAD, colitis-associated dysplasia; GTPase, guanosine 5'-triphosphate hydrolase; HGF, hepatocyte growth factor; HIPPO, Salvador-Warts-Hippo signaling pathway; IPA, ingenuity pathway analysis; LS, left-sided colitis; p53, tumour protein P53; Pan, pancolitis; PD, programmed death; PD-L, programmed death ligand; PPAR, peroxisome proliferator–activated receptor; Rac, Rac family small GTPases; Rho, Rho family small GTPases; RhoGDI, Rho guanosine 5'-diphosphate dissociation inhibitor; RXR, retinoid X receptor; UC, ulcerative colitis (See online version for color figure).

Differential Correlation of DAPK3-YAP with UC Disease Progression

Given the association of Hippo signaling activation with the UC extent (Figure 3A), and the implication of *DAPK3* and *PPP1CB* as key factors in colitis-dysplasia progression (Figure 5), differential correlation analyses for the pairings *DAPK3-YAP* and *PPP1CB-YAP* were conducted to assess potential differences in gene-gene regulatory relationships among the UC disease subtypes. The GSE47908 data set was generated using 3 probe sets for *DAPK3* (Figure S1A), 3 probe sets for *YAP* (Figure S1B), and 4 probe sets for *PPP1CB* (Figure S1C). Resolution of probe set redundancy with the IPA software returned 1 representative probe set each for *DAPK3* (203890_s_at) and *PPP1CB* (228222_at); however, 2 representative probe sets (213342_at and 224894_at) were resolved for *YAP*. To identify the *YAP* probe set that best satisfied the assumption of a Pearson correlation, in which the expression values represented by the probe sets are normally distributed, the Shapiro-Wilk test was performed separately for each probe set. Expression values represented by 2 of the 3 *YAP* probe sets (213342_at and 224894_at) conformed to a normal distribution (i.e., $P > .05$ across all conditions). Additionally, expression values represented by probe set 2133342_at returned a higher mean W value (0.948 versus 0.940 for 213342_at and 224894_at, respectively). As such, expression values represented by probe set 213342_at were utilized for the subsequent Pearson correlation analysis. The Shapiro-Wilk test was also performed for the *DAPK3* and *PPP1CB* probe sets. While the representative *DAPK3* probe set selected by IPA (203890_s_at) passed the test of normality (Figure S1A), the representative probe set selected by IPA for *PPP1CB* (228222_at) did not (i.e., with $P < .05$ for left-sided colitis, the null hypothesis of normality was rejected; Figure S1C). Because the *PPP1CB* expression values did not display a normal distribution, the Pearson's correlation test could not be used for population inferences. However, a relationship between the expression of *PPP1CB* and *YAP* for this sample set could still be inferred. As such, for the sake of continuity, expression values derived from probe set 228222_at were used to study whether there was some association between the expression of *PPP1CB* and *YAP* and to estimate the strength of this relationship.

As shown in Figure 6A, the *DAPK3-YAP* correlation in healthy controls was negative but flipped to positive in left-sided colitis. Moreover, as the UC disease extent progressed from left-sided colitis to pancolitis and then on to CAD, the *DAPK3-YAP* correlation grew progressively more positive. The general direction of the differential correlation for the *PPP1CB-YAP* pairing mirrors that of the *DAPK3-YAP* pairing (Figure 6B). However, the differential correlation with the UC disease extent was less apparent for the *PPP1CB-YAP* pairing. This result suggests that changes in the potential regulatory relationship between DAPK3 and YAP, conditioned on the UC disease extent, may contribute to disease progression.

Discussion

In UC, a prolonged disease duration and extensive intestinal involvement (i.e., pancolitis) are associated with an increased risk for colorectal cancer.[12] The progression of carcinogenesis

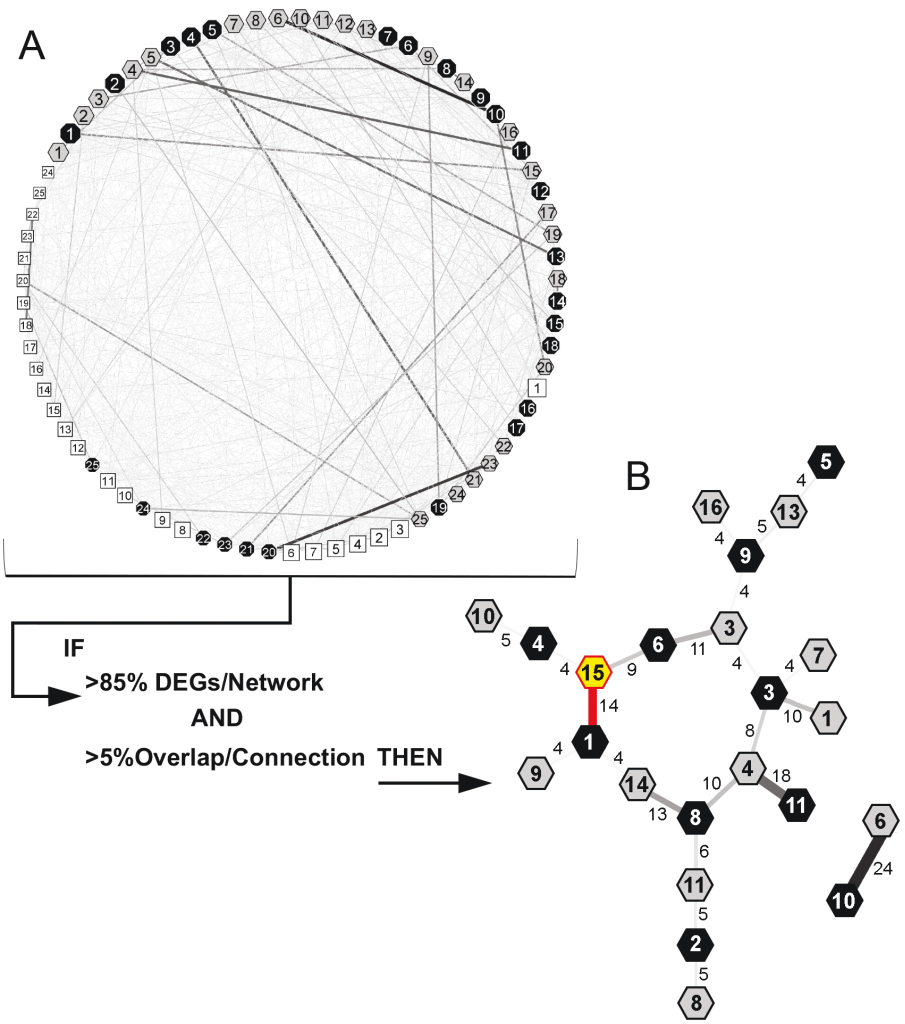

Figure 4. Intersections of UC clinical subtype molecular interactions. Molecular networks were constructed for each UC subtype. Octagons represent networks constructed with CAD DEGs, hexagons represent pancolitis networks, and rectangles indicate left-sided colitis networks. The shape size represents the relative number of DEGs used to build each network. The networks are connected to each other if there are any overlapping gene products, and line widths represent the numbers of shared gene products. A, The serpentine network overlap was detangled by focusing on networks that had >85% of DEG inputs and keeping edges that involved >5% overlap of gene products. B, This returned a core network of networks that was heavily leveraged on the edge connecting CAD network 1 and pancolitis network 15 (red). Abbreviations: CAD, colitis-associated dysplasia; DEG, differentially expressed gene; UC, ulcerative colitis (See online version for color figure).

in UC is thought to be driven by chronic inflammation and proceeds in a stepwise manner through a colitis-dysplasia-carcinoma sequence.[5,6] As the area affected by UC grows, so too does the inflammatory load, which could in turn accelerate dysplasia and CAC tumorigenesis.[17] While the impact that inflammation can have on colon carcinogenesis should not be discounted, evidence also suggests that noninflammatory factors play a role in mediating the colitis-dysplasia-carcinoma progression.[7,17,18] Among patients or animals with similar inflammatory statuses, some develop CAC, while others do not.[7] Additionally, a whole-exome sequence analysis of IBD-associated colorectal cancer showed that apart from rare cases of mutations in DNA proofreading or repair pathways, supra-IBD inflammation alone does not compel greater mutation rates when compared with sporadic CRC of a noninflammatory origin.[18] This also supports a role for noninflammatory factors in mediating colitis-dysplasia-carcinoma progression. As an example, azoxymethane -treated *IL10-/-* mice infected with colitogenic *Escherichia coli* NC101 or *Enterococcus faecalis* OG1RF exhibited similar degrees of colitis and comparable levels of immune infiltrate; tumors were only observed in 10% of *E. faecalis*–infected mice, whereas 80% of *E. coli*–infected mice showed tumor development. The polyketide synthase genotoxic island, found in *E. coli* NC101 but not *E. faecalis* OG1RF, was linked to the DNA damage and subsequent tumorigenesis in the *E. coli*–infected mice.[19] Moreover, gene mutation and gene expression analyses have linked cytoskeleton remodeling to colitis-dysplasia-carcinoma progression.[18,20,21] Our investigation verified pancolitis as a conduit for UC advancement from left-sided colitis to CAD and confirmed dysregulation of actin reorganization as a key determinant for the progression of UC from nondysplastic to dysplastic UC.

Bjerrum et al.[13] previously defined distinct gene expression signatures for dysplasia versus pancolitis, dysplasia versus left-sided UC, and pancolitis versus left-sided UC in the GSE47908 data set. These expression signatures manifested GO terms for left-sided UC (i.e., protein metabolic process

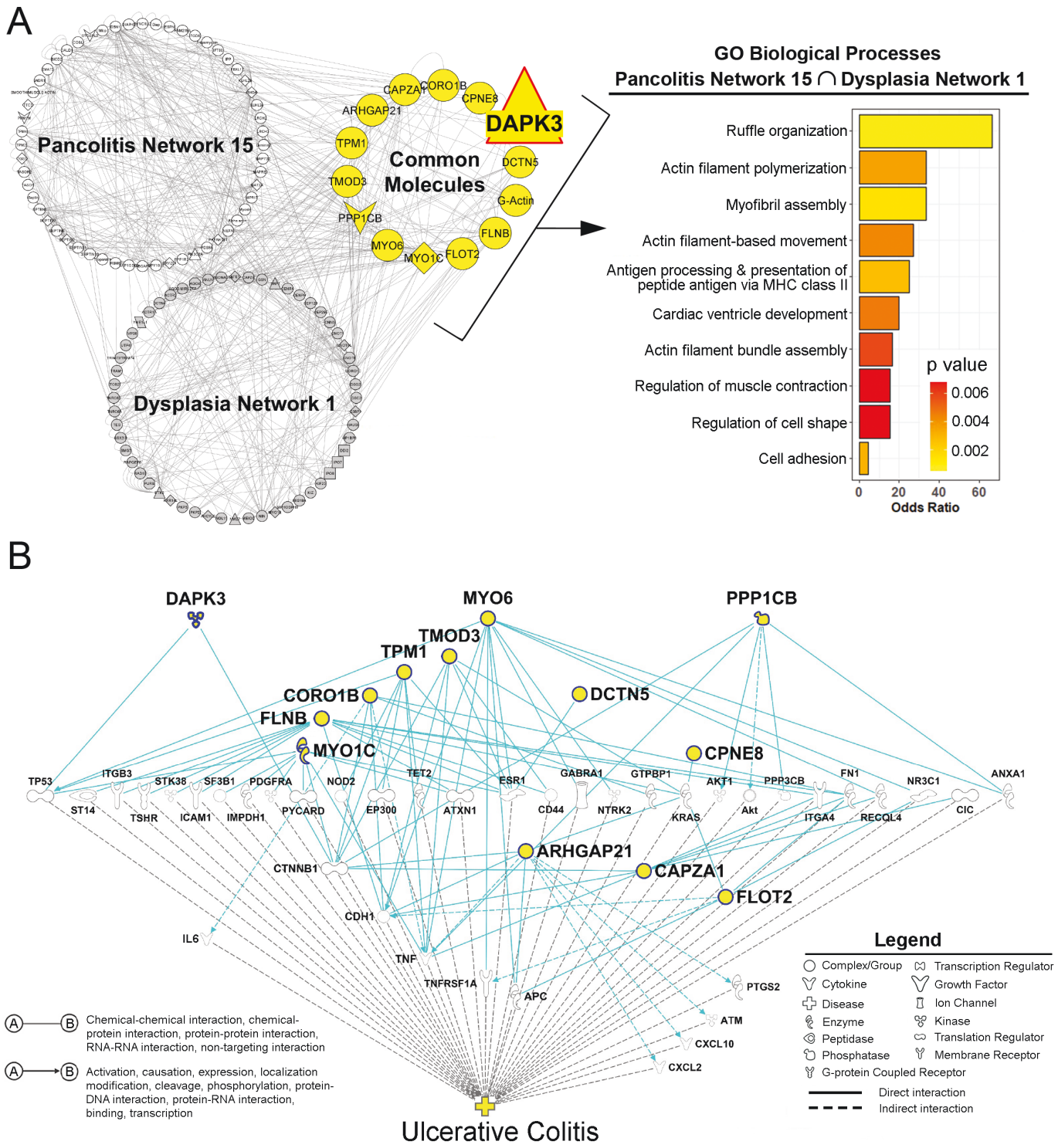

Figure 5. Gene ontology term enrichment analysis of the pancolitis network 15 and CAD network 1 intersection. A, Differentially expressed genes at the intersection of pancolitis network 15 ∩ CAD network 1 were subjected to a GO term enrichment analysis for Biological Process categories. The network was constructed by IPA software, and intersections were compiled with RVenn R. Edge-betweenness was computed by the Cytoscape app NetworkAnalyzer. Enrichment was performed with topGO R. Statistical significance was defined with a Fisher's exact test. B, The shortest paths linking the 13 focus molecules to UC were established using the IPA Path Explorer tool. The 13 focus molecules (highlighted in yellow) were used as the starting point for the generation of biological networks based on their connectivity as established in the IKB. Incorporating findings from experimentally observed or highly predicted confidence levels and direct or indirect interactions, the IPA Path Explorer tool built the 88 shortest paths to connect focus molecules through a minimum of 1 IPA-derived intermediate molecule to UC. All probable shortest paths by which the focus molecules were connected to UC required at least 1 interconnecting gene product (i.e., none of the lines originating from any of the focus molecules [colored in light blue] connect directly to UC). Abbreviations: CAD, colitis-associated dysplasia; DAPK3, death-associated protein kinase 3; DEG, differentially expressed gene; GO, gene ontology; IKB, Ingenuity Knowledge Base; MHC, major histocompatibility complex; UC, ulcerative colitis (See online version for color figure).

Table 1. Overlapping gene products in the pancolitis 15 ∩ CAD network 1 intersection.[a]

Gene	Protein	Molecular function	Expression FC		
			L	P	D
DAPK3	Death-associated protein kinase 3	Kinase	−0.15	−1.08[b]	−0.98[b]
PPP1CB	Protein phosphatase PP1β subunit	Phosphatase	−0.12	−1.56[b]	−1.52[b]
MYO1C	Unconventional myosin IC	Motor	−0.18	0.77[c]	0.99[c]
MYO6	Unconventional myosin VI	Motor	−0.31	−0.88[b]	−1.36[b]
ARHGAP21	Rho GTPase-activating protein 21	GTPase	−0.48	−0.98[b]	−0.97[b]
CAPZA1	F-actin-capping protein α1	Actin Binding	0.18	−1.89[b]	−2.21[b]
CORO1B	Coronin 1B	Actin Binding	−0.08	0.88[c]	0.86[c]
CPNE8	Copine 8	Membrane Binding	−0.34	−1.55[b]	−1.93[b]
DCTN5	Dynactin 5	Scaffold	−0.20	−0.80[b]	−1.64[b]
FLNB	Filamin B	Actin Binding	−0.49	−0.76[b]	−1.20[b]
FLOT2	Flotillin 2	Scaffold	0.17	−0.78[b]	−0.95[b]
TMOD3	Tropomodulin 3	Actin Binding	−0.22	−1.36[b]	−2.15[b]
TPM1	Tropomyosin α1	Actin Binding	−0.61	−0.86[b]	1.01[c]
—	Monomeric (G) actin	Structural	Not a focus molecule		

[a] A gene was deemed dysregulated when the FC is >0.75 and FDR is <0.001. Abbreviations: CAD, colitis-associated dysplasia; D, colitis-associated dysplasia; FC, $\log_2$ fold-change; FDR, false discovery rate; GTPase, guanosine 5'-triphosphate hydrolase; L, left-sided colitis; P, pancolitis; PP1, protein phosphatase type-1.
[b] Significant downregulation.
[c] Significant upregulation.

and cell cycle process) that distinguished the early disease stage from pancolitis and dysplasia (i.e., protein export from nucleus and response to insulin stimulus). Our output of GO enrichment terms identifies the dysregulation of inflammatory processes to exist at the intersection of pancolitis and left-sided UC. These terms were excluded from the original Bjerrum et al.[13] analysis, since statistical filtering was employed to eliminate DEGs that were solely reflective of inflammation. In addition, our inquiry also uniquely revealed that the intersection of pancolitis with CAD was rooted in the dysregulation of actin-based processes (i.e., actin cytoskeleton reorganization and microvillus assembly). Bjerrum et al.[13] further extracted a panel of transcripts for therapeutic importance based on their known involvement in inflammatory and neoplastic processes; mitogen-activated protein-kinase-interacting serine/threonine protein kinase 2 (*MKNK2*) and insulin receptor alpha (*INSRA*) were authenticated as potential critical transcripts for inflammation-driven tumorigenesis. Laminin γ2 was also highlighted as a biomarker of preneoplastic lesions in UC that still awaits validation. In our analyses, these DEGs also exist solely within specific disease types (Table S1); their absence from the DEG networks that bridge pancolitis and CAD suggests that distinct signaling mechanisms are responsible for the progression and the maintenance of disease states.

Subsequent to the Bjerrum et al.[13] study, the GSE47908 data set was also used by investigators to interrogate key genes and/or biological processes in the context of UC progression. Most commonly, GSE47908 was combined with other data sets from the GEO to conduct a differential expression comparison of UC versus normal samples. As an example, Kaiko and colleagues[22] included GSE47908 as part of their multi-institute, retrospective cohort study, which identified plasminogen activator inhibitor 1 as a link between the epithelium and inflammation. Unfortunately, when these studies consolidated GSE47908 with other GEO datasets, the key strength of GSE47908 was inadvertently lost. That is, the extent of disease, which may affect transcriptional profiles, was no longer accounted for.

The prominent positioning of actin-based processes within the network intersection of pancolitis and CAD (Figure 5) substantiates results of a gene expression analysis of patients with CAC, presented by Kanaan and colleagues,[20] that established actin cytoskeleton organization as the most significantly disrupted process in UC progression. A protein abundance analysis of UC progressors (UC patients with CAD or CAC) versus nonprogressors has also identified enrichment of dysregulated cytoskeletal proteins in UC progressors.[23] Drawbacks in these 2 studies include the evaluation of UC progression in a binary fashion (presence or absence of CAD and/or CAC) and the small sample sizes (i.e., 3 unique patients in the study conducted by Kanaan and colleagues[20] and 15 unique patients in the study conducted by May and colleagues[23]). To provide insight into the molecular events associated with the stepwise progression of UC, it will be necessary to demonstrate that the dysregulations observed in CAD or CAC were issued forth from some form of nondysplastic UC.

Signal transduction pathways regulate many cellular functions that were found to be altered in UC carcinogenesis, such as proliferation, growth, differentiation, metabolism, and survival. Molecular investigations have previously associated signal transducer and activator of transcription 3 (STAT3), Wingless-related integration site (Wnt), transforming growth factor β, and toll-like receptor 4 or nuclear transcription factor κB signaling with the pathogenesis of colon carcinogenesis.[24–26] However, the pathways most relevant to the gene expression changes observed during the early progression of UC, before any histological evidence of dysplasia or carcinoma, remain unknown. In this regard, Hippo signaling and Ephrin-receptor signaling were uncovered as the top canonical pathways that were progressively

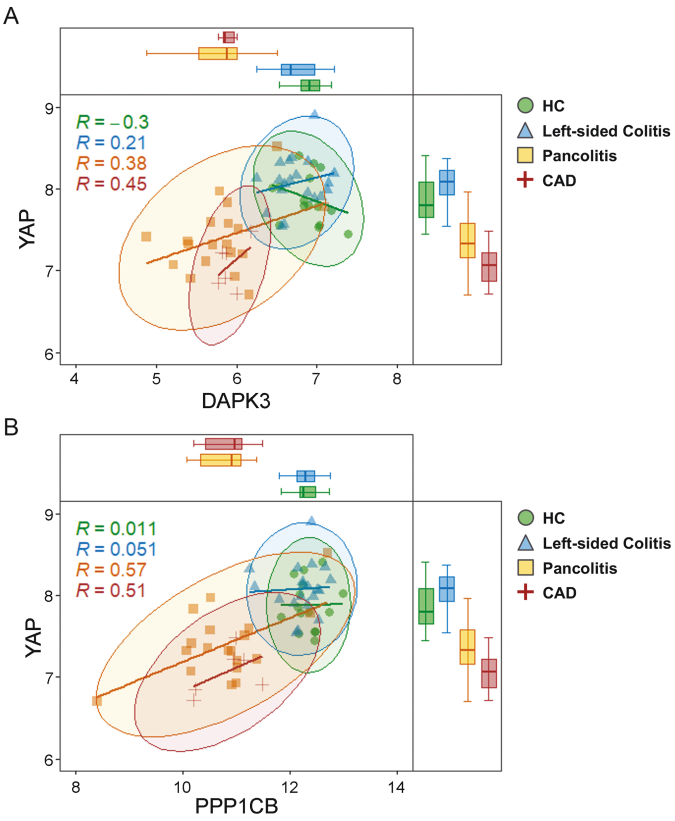

Figure 6. Differential correlation of *DAPK3-YAP* and *PPP1CB-YAP* relationships. The main panels display the relationships between the log-transformed expression profiles of (A) *DAPK3* and *YAP* or (B) *PPP1CB* and *YAP*. These scatterplots are overlayed with confidence ellipses of covariance, constructed for the 95% CI. In the marginal box plots of log-transformed gene expression, the lower whisker represents the lowest datum still within 1.5 times the IQR of the lower quartile, and the upper whisker represents the highest datum still within 1.5 times the IQR of the upper quartile. Abbreviations: CAD, colitis-associated dysplasia; CI, confidence interval; DAPK3, death-associated protein kinase 3; HC, healthy controls; IQR, interquartile range; PPP1CB, protein phosphatase PP1β catalytic subunit; YAP, Yes-associated protein.

altered in concert with the extent of UC progression (Figure 3A). The Hippo pathway is a fundamental signaling cascade that negatively regulates the activity of YAP or the transcriptional coactivator with PDZ-binding motif (TAZ) to coordinate cell proliferation, apoptosis, and cell movement; as such, it is essential for tissue homeostasis, repair, and regeneration.[27] Importantly, YAP- or TAZ-mediated cell proliferation in epithelial monolayers is controlled by a cytoskeletal checkpoint that, in turn, is monitored by actin-processing factors. The Ephrin pathway also controls intestinal homeostasis through cell proliferation and cell movement, additionally to cell attachment and repulsion.[28,29] However, deciphering functional outcomes by Ephrin-pathway activation is circuitous due to the redundancy and idiosyncrasy of this pathway.[30] The Ephrin receptors (Eph) comprise the largest family of receptor tyrosine kinases (RTKs). But, unlike most RTKs, for which ligands are generally soluble, the cognate ligands of Eph receptors, the ephrins, are also membrane bound. This aspect of the Eph-ephrin receptor-ligand pairing consequently induces bidirectional signaling, where signaling through Eph is termed forward signaling and signaling through ephrin is termed reverse signaling. Furthermore, there is a plethora of Ephs and ephrins (i.e., 14 Ephs, 8 ephrins) with promiscuous pairing options. Eph or ephrin also exhibits *cis* interactions to inhibit forwarding signaling. Ephrin is therefore a more convoluted pathway to render (Figure S3), relative to the Hippo pathway (Figure S2).

The Hippo pathway was previously identified as a key factor for the compensatory regeneration of intestinal epithelial cells in response to tissue injury using a colitis mouse model.[31] The recent emergence of YAP as a potential regulator of intestinal diseases involves elements beyond the canonical Hippo pathway. For 1, YAP can be sequestered at adherens junctions via interactions with α-catenin,[32] the abundance of which is significantly altered in active UC.[33] Secondly, nuclear translocation of YAP may be brought about via stimulation of gp130-associated Src family kinase Yes.[34] Finally, YAP was found to be a crucial pivot point of cellular reprograming during intestinal epithelial repair, coupling epithelial restitution to the proliferative phase of regeneration by way of focal adhesion kinase (FAK)-Src signaling.[35] In view of YAP as a mechanosensor and mechanotranducer amidst epithelial regeneration of injured tissue, a comprehensive understanding of the interplay between YAP and the actin cytoskeleton is needed to make rational selections of therapeutic targets for patients at high risk of UC neoplastic progression.

The identification of DAPK3 as a potential key factor in UC progression is particularly interesting. Death-associated protein kinase 3 was shown to influence the proliferation of colon cancer cells[36]; however, a role for DAPK3 in UC pathogenesis (i.e., within the context of colitis or colitis-associated dysplasia-carcinoma) was unknown prior to this study. Death-associated protein kinase 1, the closely related family member and upstream regulator of DAPK3, was previously associated with UC severity[37] and gastrointestinal cancer pathogenesis.[38] In addition, pharmacological inhibition of DAPK1 was reported to augment susceptibility to dextran sodium sulfate (DSS)-induced colitis in mice, with a concomitant increase in bacterial translocation ascribed to epithelial barrier defects.[39] It is regrettable that the small molecule inhibitor of DAPK1 (i.e., DAPK6) applied in the study of tunicamycin (TM)-induced, endoplasmic reticulum (ER)-stress-dependent reduction of bacterial translocation, potently cross-inhibits DAPK3 (IC_{50} = 225 nM[40]) and Rho-associated coil-coiled kinase (ROCK; K_i = 132 nM[41]). Although the Lopes et al.[39] study included small interfering RNA (siRNA) knockdown experiments to independently validate DAPK1 signaling involvement, the potential impact of concurrent DAPK3 and ROCK inhibition brought forth with the DAPK6 inhibitor was not examined. Previously, Ito and colleagues[42] showed that ROCK activity increased in response to TM, and that treatment with Y27632 (a selective ROCK inhibitor) completely reversed TM-induced ER-stress responses in the J774 macrophage cell line. Moreover, the involvement of DAPK3 in the ER-stress response was also demonstrated in human aortic vascular smooth muscle cells, where short hairpin RNA (shRNA)-mediated silencing of *DAPK3* ablated the calcifying-media-induced increase of CCAAT-enhancer-binding protein homologous protein (CHOP), a multifunctional transcription factor in the ER-stress response.[43] In the same study, treatment with DAPK6 attenuated vascular calcification in rats, alongside a significant reduction in the CHOP protein abundance in the

aorta. It may be beneficial to learn whether DAPK3 and/or ROCK alter ER-stress-dependent autophagy in the context of DSS-induced colitis in mice.

Some limitations in the present study are apparent. First, the progression of UC to CAD occurs through multiple mechanisms involving various cell types. The analyses were completed on transcriptional profiles generated from mucosal biopsies, and genes may demonstrate diverse functions across different cell types. Hence, the gene sets identified from the averaged tissue data set will require re-examination in a cell type–specific way (e.g., single-cell RNA-Seq) to precisely identify the susceptible cell types and convergent pathways among different cells. Second, we were unable to identify additional publicly available data sets that specifically assessed gene expression in inflamed (involved) colon tissues of UC patients with adequate control for the relationship between the colonic biopsy location and gene expression. Five data series (i.e., GSE37283,[44] GSE38713,[45] GSE48634,[46] GSE105074,[47] and GSE87466[48]) were considered as potential verification and comparison cohorts since these possess gene expression data for colonic biopsies obtained from HC and UC patients grouped by disease extension (i.e., left-sided colitis versus pancolitis). Unfortunately, GSE48634, GSE105074, and GSE87466 were eliminated as appropriate verification data sets due to critical differences in the locations and inflammatory statuses of biopsies. In these cases, the biopsy location was associated with greater variation than disease extent (Figure S4). However, *DAPK3* expression in the GSE38713 data series was significantly downregulated in left-sided colitis (FC = –1.42; FDR = 0.006; remission involved biopsies), as well as in pancolitis (FC = –1.74; FDR = 0.04; remission involved biopsies). A differential correlation analysis of *DAPK3-YAP* expression across the active involved groupings showed a loss of relationship between *DAPK3* and *YAP* as the disease transitioned from normal to left-sided active involvement, and then to pancolitis active involvement (Figure S5). In addition, a negative correlation for *DAPK3-YAP* was corroborated in HC of the GSE37283 data set.[44] The relationship flipped to positive in UC patients harboring a remote neoplastic lesion (Figure S6), confirming the *DAPK3-YAP* relationships identified in the Bjerrum et al.[13] data series (Figure 6A). Finally, the results of this study represent a data mining activity, so additional, well-designed investigations will be required for validation of findings. Despite these drawbacks, independent confirmations and similarities among verification cohorts provide a high level of confidence in the overall significance of *DAPK3* and *YAP* in UC neoplastic progression.

Conclusions

The probability that DAPK3 plays a role in the progression of the pathological changes of UC is notable. To substantiate the connection of DAPK3 to UC progression, the difference in correlations between *DAPK3* and *YAP* was studied in all UC clinical subtypes plus HC samples. Differential coexpression operates on the level of gene pairs and is used as an alternative approach to identify disease-related genes.[49] Results from the differential coexpression analyses demonstrate the correspondence of the *DAPK3-YAP* correlation and the UC extent. This suggests that changes in the potential regulatory relationship between DAPK3 and YAP, conditioned on the UC extent, may contribute to UC progression. Still, the drivers behind the differential *DAPK3-YAP* coexpression pattern are unclear. Better understanding of the relationship between YAP and DAPK3 may enable the discovery of targeted therapy for the prevention of UC neoplastic progression.

Supplementary Data

Supplementary data are available at *Inflammatory Bowel Diseases* online.

Author Contributions

H.-M.C. completed the data analysis, prepared the figures, and wrote the manuscript. J.A.M. conceived and coordinated the study, wrote the manuscript, supervised trainees, and provided intellectual contributions to the project. Both authors reviewed the results and approved the final version of the manuscript.

Funding

This work was supported by a research grant from the Canadian Institutes of Health Research (MOP#97931 to J.A.M.). H.-M.C. was a recipient of the Canadian Institutes of Health Research Fredrick Banting and Charles Best Canada and Alberta Graduate Excellence Scholarships.

Conflicts of Interest

J.A.M. is cofounder of and has an equity position in Arch Biopartners Inc.

References

1. Ordas I, Eckmann L, Talamini M, Baumgart DC, Sandborn WJ. Ulcerative colitis. *Lancet*. 2012;380(9853):1606–1619.
2. Porter RJ, Kalla R, Ho GT. Ulcerative colitis: recent advances in the understanding of disease pathogenesis. *F1000Research*. 2020;9.
3. Younis N, Zarif R, Mahfouz R. Inflammatory bowel disease: between genetics and microbiota. *Mol Biol Rep*. 2020;47(4):3053–3063.
4. Jostins L, Ripke S, Weersma RK, et al. Host-microbe interactions have shaped the genetic architecture of inflammatory bowel disease. *Nature*. 2012;491(7422):119–124.
5. Dulai PS, Sandborn WJ, Gupta S. Colorectal cancer and dysplasia in inflammatory bowel disease: a review of disease epidemiology, pathophysiology, and management. *Cancer Prev Res (Phila)*. 2016;9(12):887–894.
6. Low D, Mino-Kenudson M, Mizoguchi E. Recent advancement in understanding colitis-associated tumorigenesis. *Inflamm Bowel Dis*. 2014;20(11):2115–2123.
7. Van Der Kraak L, Gros P, Beauchemin N. Colitis-associated colon cancer: is it in your genes? *World J Gastroenterol*. 2015;21(41):11688–11699.
8. Kabir M, Fofaria R, Arebi N, et al. Systematic review with meta-analysis: IBD-associated colonic dysplasia prognosis in the videoendoscopic era (1990 to present). *Aliment Pharmacol Ther*. 2020;52(1):5–19.
9. Ananthakrishnan AN, Cagan A, Cai T, et al. Colonoscopy is associated with a reduced risk for colon cancer and mortality in patients with inflammatory bowel diseases. *Clin Gastroenterol Hepatol*. 2015;13(2):322–329.e321.
10. Ullman T, Odze R, Farraye FA. Diagnosis and management of dysplasia in patients with ulcerative colitis and Crohn's disease of the colon. *Inflamm Bowel Dis*. 2009;15(4):630–638.

11. Baker AM, Cross W, Curtius K, et al. Evolutionary history of human colitis-associated colorectal cancer. *Gut*. 2019;68(6):985–995.
12. Zhou Q, Shen ZF, Wu BS, et al. Risk of colorectal cancer in ulcerative colitis patients: a systematic review and meta-analysis. *Gastroenterol Res Pract*. 2019;2019:5363261.
13. Bjerrum JT, Nielsen OH, Riis LB, et al. Transcriptional analysis of left-sided colitis, pancolitis, and ulcerative colitis-associated dysplasia. *Inflamm Bowel Dis*. 2014;20(12):2340–2352.
14. Ritchie ME, Phipson B, Wu D, et al. *limma* powers differential expression analyses for RNA-sequencing and microarray studies. *Nucleic Acids Res*. 2015;43(7):e47.
15. Newman ME, Girvan M. Finding and evaluating community structure in networks. *Phys Rev E*. 2004;69(2 Pt 2):026113.
16. Yoon J, Blumer A, Lee K. An algorithm for modularity analysis of directed and weighted biological networks based on edge-betweenness centrality. *Bioinformatics*. 2006;22(24):3106–3108.
17. Grivennikov SI, Cominelli F. Colitis-associated and sporadic colon cancers: different diseases, different mutations? *Gastroenterology*. 2016;150(4):808–810.
18. Robles AI, Traverso G, Zhang M, et al. Whole-exome sequencing analyses of inflammatory bowel disease-associated colorectal cancers. *Gastroenterology*. 2016;150(4):931–943.
19. Arthur JC, Perez-Chanona E, Muhlbauer M, et al. Intestinal inflammation targets cancer-inducing activity of the microbiota. *Science*. 2012;338(6103):120–123.
20. Kanaan Z, Qadan M, Eichenberger MR, Galandiuk S. The actin-cytoskeleton pathway and its potential role in inflammatory bowel disease-associated human colorectal cancer. *Genet Test Mol Biomarkers*. 2010;14(3):347–353.
21. Majumdar D, Tiernan JP, Lobo AJ, Evans CA, Corfe BM. Keratins in colorectal epithelial function and disease. *Int J Exp Pathol*. 2012;93(5):305–318.
22. Kaiko GE, Chen F, Lai CW, et al. PAI-1 augments mucosal damage in colitis. *Sci Transl Med*. 2019;11(482):eaat0852.
23. May D, Pan S, Crispin DA, et al. Investigating neoplastic progression of ulcerative colitis with label-free comparative proteomics. *J Proteome Res*. 2011;10(1):200–209.
24. Claessen MM, Schipper ME, Oldenburg B, Siersema PD, Offerhaus GJ, Vleggaar FP. WNT-pathway activation in IBD-associated colorectal carcinogenesis: potential biomarkers for colonic surveillance. *Cell Oncol*. 2010;32(4):303–310.
25. Muller M, Hansmannel F, Arnone D, et al. Genomic and molecular alterations in human inflammatory bowel disease-associated colorectal cancer. *United European Gastroenterol J*. 2020;8(6):675–684.
26. Tang A, Li N, Li X, et al. Dynamic activation of the key pathways: linking colitis to colorectal cancer in a mouse model. *Carcinogenesis*. 2012;33(7):1375–1383.
27. Park J, Hansen CG. Cellular feedback dynamics and multilevel regulation driven by the hippo pathway. *Biochem Soc Trans*. 2021;49(4):1515–1527.
28. Grandi A, Zini I, Palese S, et al. Targeting the Eph/Ephrin system as anti-inflammatory strategy in IBD. *Front Pharmacol*. 2019;10:691.
29. Perez White BE, Getsios S. Eph receptor and ephrin function in breast, gut, and skin epithelia. *Cell Adh Migr*. 2014;8(4):327–338.
30. Arvanitis D, Davy A. Eph/ephrin signaling: networks. *Genes Dev*. 2008;22(4):416–429.
31. Cai J, Zhang N, Zheng Y, de Wilde RF, Maitra A, Pan D. The Hippo signaling pathway restricts the oncogenic potential of an intestinal regeneration program. *Genes Dev*. 2010;24(21):2383–2388.
32. Schlegelmilch K, Mohseni M, Kirak O, et al. Yap1 acts downstream of alpha-catenin to control epidermal proliferation. *Cell*. 2011;144(5):782–795.
33. Karayiannakis AJ, Syrigos KN, Efstathiou J, et al. Expression of catenins and E-cadherin during epithelial restitution in inflammatory bowel disease. *J Pathol*. 1998;185(4):413–418.
34. Taniguchi K, Wu LW, Grivennikov SI, et al. A gp130-Src-YAP module links inflammation to epithelial regeneration. *Nature*. 2015;519(7541):57–62.
35. Yui S, Azzolin L, Maimets M, et al. YAP/TAZ-dependent reprogramming of colonic epithelium links ECM remodeling to tissue regeneration. *Cell Stem Cell*. 2018;22(1):35–49.e37.
36. Togi S, Ikeda O, Kamitani S, et al. Zipper-interacting protein kinase (ZIPK) modulates canonical Wnt/beta-catenin signaling through interaction with Nemo-like kinase and T-cell factor 4 (NLK/TCF4). *J Biol Chem*. 2011;286(21):19170–19177.
37. Kuester D, Guenther T, Biesold S, et al. Aberrant methylation of DAPK in long-standing ulcerative colitis and ulcerative colitis-associated carcinoma. *Pathol Res Pract*. 2010;206(9):616–624.
38. Yuan W, Chen J, Shu Y, et al. Correlation of DAPK1 methylation and the risk of gastrointestinal cancer: a systematic review and meta-analysis. *PLoS One*. 2017;12(9):e0184959.
39. Lopes F, Keita AV, Saxena A, et al. ER-stress mobilization of death-associated protein kinase-1-dependent xenophagy counteracts mitochondria stress-induced epithelial barrier dysfunction. *J Biol Chem*. 2018;293(9):3073–3087.
40. Okamoto M, Takayama K, Shimizu T, Ishida K, Takahashi O, Furuya T. Identification of death-associated protein kinases inhibitors using structure-based virtual screening. *J Med Chem*. 2009;52(22):7323–7327.
41. Al-Ghabkari A, Deng JT, McDonald PC, et al. A novel inhibitory effect of oxazol-5-one compounds on ROCKII signaling in human coronary artery vascular smooth muscle cells. *Sci Rep*. 2016;6:32118.
42. Ito H, Yamashita Y, Tanaka T, et al. Cigarette smoke induces endoplasmic reticulum stress and suppresses efferocytosis through the activation of RhoA. *Sci Rep*. 2020;10(1):12620.
43. Li KX, Du Q, Wang HP, Sun HJ. Death-associated protein kinase 3 deficiency alleviates vascular calcification via AMPK-mediated inhibition of endoplasmic reticulum stress. *Eur J Pharmacol*. 2019;852:90–98.
44. Pekow J, Dougherty U, Huang Y, et al. Gene signature distinguishes patients with chronic ulcerative colitis harboring remote neoplastic lesions. *Inflamm Bowel Dis*. 2013;19(3):461–470.
45. Planell N, Lozano JJ, Mora-Buch R, et al. Transcriptional analysis of the intestinal mucosa of patients with ulcerative colitis in remission reveals lasting epithelial cell alterations. *Gut*. 2013;62(7):967–976.
46. Smith PJ, Levine AP, Dunne J, et al. Mucosal transcriptomics implicates under expression of BRINP3 in the pathogenesis of ulcerative colitis. *Inflamm Bowel Dis*. 2014;20(10):1802–1812.
47. Vinayaga-Pavan M, Frampton M, Pontikos N, et al. Elevation in cell cycle and protein metabolism gene transcription in inactive colonic tissue from Icelandic patients with ulcerative colitis. *Inflamm Bowel Dis*. 2019;25(2):317–327.
48. Li K, Strauss R, Ouahed J, et al. Molecular comparison of adult and pediatric ulcerative colitis indicates broad similarity of molecular pathways in disease tissue. *J Pediatr Gastroenterol Nutr*. 2018;67(1):45–52.
49. McKenzie AT, Katsyv I, Song WM, Wang M, Zhang B. DGCA: a comprehensive R package for differential gene correlation analysis. *BMC Syst Biol*. 2016;10(1):106.